Neuron
Article

Activity-Induced Nr4a1 Regulates Spine Density and Distribution Pattern of Excitatory Synapses in Pyramidal Neurons

Yelin Chen,[1] Yuanyuan Wang,[1] Ali Ertürk,[1] Dara Kallop,[2] Zhiyu Jiang,[1] Robby M. Weimer,[1,2] Joshua Kaminker,[3] and Morgan Sheng[1,*]
[1]Department of Neuroscience
[2]Department of Biomedical Imaging
[3]Department of Bioinformatics & Computational Biology
Genentech Inc, South San Francisco, CA 94080, USA
*Correspondence: sheng.morgan@gene.com
http://dx.doi.org/10.1016/j.neuron.2014.05.027

SUMMARY

Excitatory synapses occur mainly on dendritic spines, and spine density is usually correlated with the strength of excitatory synaptic transmission. We report that *Nr4a1*, an activity-inducible gene encoding a nuclear receptor, regulates the density and distribution of dendritic spines in CA1 pyramidal neurons. Nr4a1 overexpression resulted in elimination of the majority of spines; however, postsynaptic densities were preserved on dendritic shafts, and the strength of excitatory synaptic transmission was unaffected, showing that excitatory synapses can be dissociated from spines. mRNA expression profiling studies suggest that Nr4a1-mediated transcriptional regulation of the actin cytoskeleton contributes to this effect. Under conditions of chronically elevated activity, when Nr4a1 was induced, Nr4a1 knockdown increased the density of spines and PSDs specifically at the distal ends of dendrites. Thus, Nr4a1 is a key component of an activity-induced transcriptional program that regulates the density and distribution of spines and synapses.

INTRODUCTION

The majority of excitatory synapses in the mammalian brain occur on small dendritic protrusions known as spines (Nimchinsky et al., 2002). Excitatory synaptic strength correlates with spine morphology; manipulations affecting dendritic spines (density or size) or synaptic transmission often cause corresponding changes in the other. For example, overexpression of the major postsynaptic density (PSD) scaffolding proteins PSD-95 or Shank enhances synaptic transmission as well as increases spine size and/or density (El-Husseini et al., 2000; Sala et al., 2001). Conversely, pathological conditions often cause reduction of both spine size/density and synaptic transmission, including exposure of neurons to amyloid-β (Hsieh et al., 2006).

Synaptic plasticity, the functional and morphological modification of synapses, is crucial for brain development and cognitive functions like learning and memory. Spine structural plasticity correlates well with synaptic plasticity (Hayashi and Majewska, 2005; Holtmaat and Svoboda, 2009). Long-term potentiation (LTP) stimulation induces spine enlargement (Kopec et al., 2006; Lang et al., 2004; Matsuzaki et al., 2004), while long-term depression (LTD) is associated with spine shrinkage (Nägerl et al., 2004; Zhou et al., 2004).

The most-studied form of synaptic plasticity—early phase LTP in hippocampus—requires activation of N-methyl-D-aspartate receptors (NMDARs) and involves trafficking of existing AMPA receptors (AMPARs). Long-lasting forms of synaptic plasticity such as late-phase LTP (L-LTP) require additionally transcription and translation. The cAMP response-element-binding protein (CREB) is a transcription factor activated by NMDARs that is necessary for maintenance of L-LTP, suggesting that CREB-induced genes play a role in long-lasting synaptic modification (Alberini, 2009; Chen et al., 2012). Transcriptional mechanisms are also implicated in activity-induced synapse elimination. Activation of transcription factor Myocyte enhancing factor 2 (MEF2) by neuronal activity results in synapse elimination, whereas loss of MEF2 function in neurons leads to increased synapse number (Barbosa et al., 2008; Flavell et al., 2006; Pulipparacharuvil et al., 2008). Thus, downstream genes controlled by MEF2 are likely to play a part in diminishing synapses in response to neuronal activity.

Nuclear receptor subfamily 4, group A, member 1 (*Nr4a1*) (also known as *NGFI-B*/*NUR77*) belongs to a family of three immediate early genes that encode three orphan nuclear receptors (Nr4a1, Nr4a2, and Nr4a3) (Hawk and Abel, 2011). In the central nervous system, Nr4a1/2/3 expression is controlled by NMDARs, CREB, and MEF2, which are key regulators of synaptic function (Benito et al., 2011; Flavell et al., 2008; Hawk and Abel, 2011; Volakakis et al., 2010; Zhang et al., 2007). Nr4a1 expression is induced by learning tasks (von Hertzen and Giese, 2005), and Nr4a1 loss-of-function causes deficits in L-LTP and long-term memory formation (Bridi and Abel, 2013; Hawk et al., 2012). Such findings suggest that Nr4a1 plays a critical role in activity-induced synaptic modification. Moreover, Nr4a family proteins are reported to protect neurons from harmful

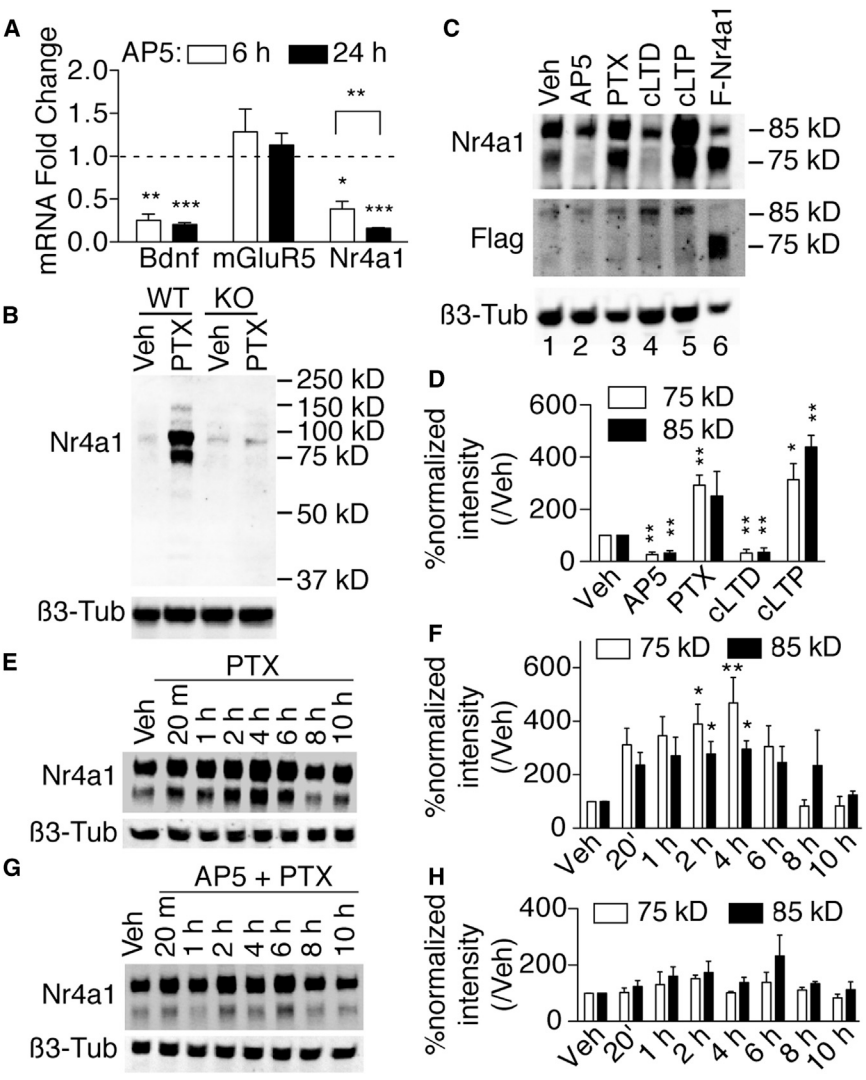

Figure 1. Regulation of Nr4a1 mRNA and Protein by NMDARs and Activity

(A) qRT-PCR of mRNA changes caused by 6 or 24 hr AP5 treatment. Fold changes are normalized to vehicle-treated controls (n = 4; Student t test).

(B) Nr4a1 immunoblot of neuron cultures from wild-type (WT) or Nr4a1 KO mice treated with vehicle control or PTX (100 μM, 4 hr). Similar results were obtained from three Nr4a1 KO mice.

(C) Nr4a1 immunoblot of neuron cultures treated with vehicle control, AP5 (100 μM, 24 hr), PTX (6 hr), cLTD (70 μM NMDA, 1 hr), cLTP (50 μM Forskolin + 0.1 μM Rolipram, 1 hr), or infected with lentivirus expressing Flag-Nr4a1 (F-Nr4a1). The same membrane was stripped and reblotted with Flag or β3-tubulin antibodies.

(D) Quantitation of (C) (n = 3, Student's t test).

(E–H) Western blot showing time course of Nr4a1 induction by PTX in the absence ([E], quantified in [F]) or presence ([G], quantified in [H]) of AP5 (n = 4, one-way ANOVA with Dunnett's multiple comparison test). All experiments were performed in dissociated hippocampal cultures (DIV18–DIV21). Error bars show SEM. *p < 0.05; **p < 0.01; ***p < 0.001.

stimuli and could be downstream effectors contributing to the neuroprotective effects of CREB (Volakakis et al., 2010; Zhang et al., 2009). The molecular and cell biological mechanisms by which Nr4a1 acts in synaptic plasticity and neuroprotection are largely unexplored.

Here, we report that overexpression of Nr4a1 eliminates dendritic spines without reducing excitatory synaptic transmission; this is achieved by preserving excitatory synapses on the dendritic shaft in the absence of spines and requires transcriptional activity of Nr4a1. This implies that spines are not necessary for excitatory synapses or excitatory transmission in pyramidal neurons. By mRNA expression profiling, we find that Nr4a1 overexpression leads to changes of numerous genes, including those in the Polo-like kinase 2 (Plk2) and RhoA/Rac1 signaling pathways, which are involved in the regulation of F-actin, the key cytoskeletal component of spines. In contrast, Nr4a1 knockdown causes excessive number of spines and PSDs to accumulate at the distal ends of dendrites, as well as impaired synaptic transmission, but only under conditions of chronic hyperactivity when Nr4a1 would be normally induced. Thus, Nr4a1 serves as an activity-induced regulator required for normal synapse distribution and function in neurons.

RESULTS

Nr4a1 Expression Is Bidirectionally Controlled by Synaptic NMDAR Activity

In neurons, mRNA of all three Nr4a genes can be induced by NMDAR and CREB activation (Barneda-Zahonero et al., 2012; Benito et al., 2011; Zhang et al., 2007). By quantitative RT-PCR (qRT-PCR), we found that Nr4a1 mRNA was reduced after 6 hr treatment of hippocampal cultures (DIV21) with NMDAR antagonist AP5 (100 μM) and further decreased after 24 hr of AP5 treatment (Figure 1A). This implies that Nr4a1 mRNA levels are maintained by basal NMDAR activity in dissociated neuronal culture. BDNF, but not mGluR5, is a known NMDAR-induced gene (Zhang et al., 2007). We found BDNF expression was also suppressed by NMDA receptor blockade of cultures in basal conditions, while mGluR5 showed no change (Figure 1A).

We next investigated whether Nr4a1 is regulated at the protein level by NMDARs and neuronal activity. By western blotting with an Nr4a1 antibody, $GABA_A$ receptor antagonist picrotoxin (PTX) (100 μM, 4 hr) induced a ~75 kDa band and an ~85 kDa band in wild-type mouse hippocampal cultures (Figure 1B). The 75 kDa and 85 kDa bands were greatly reduced in PTX-treated neuronal cultures from Nr4a1 knockout mice (Figure 1B); thus, both bands likely represent protein products of the Nr4a1 gene. The 75 kDa Nr4a1 band corresponds in size to the major Flag-tagged Nr4a1 species produced by infection of dissociated hippocampal

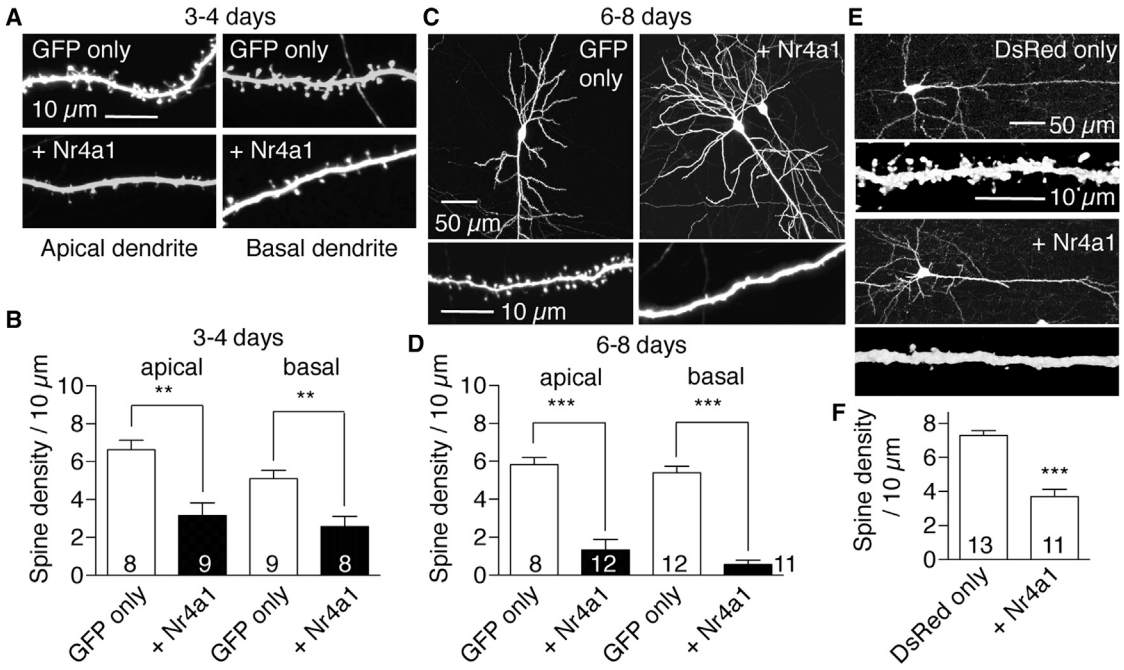

Figure 2. Overexpression of Nr4a1 Causes Loss of Dendritic Spines

(A–D) Images of live CA1 pyramidal neurons from organotypic slice cultures transfected with GFP alone or cotransfected with GFP plus Nr4a1 for 3–4 days (A) or 6–8 days (C).

(B and D) Quantitation of spine density of either apical or basal secondary dendrites from experiments shown in (A) and (C).

(E) Layer 2/3 pyramidal neurons and their dendrites from rat somatosensory cortex (2.5–3 weeks old) imaged by DsRed fluorescence, transfected in utero (E16) with either DsRed alone (upper panels) or DsRed plus Nr4a1 (lower panels).

(F) Spine density of secondary apical dendrites quantified from experiments shown in (E). Number of neurons measured for each condition is indicated in the individual bars. Error bars show SEM. Student's t test. $^{**}p < 0.01$; $^{***}p < 0.001$.

cultures with a viral vector that overexpresses Flag-Nr4a1 (F-Nr4a1), as detected with either Nr4a1 or Flag antibodies (Figure 1C, lane 6). The 85 kDa band might represent a splice variant or a posttranslationally modified form of Nr4a1 (Hazel et al., 1991).

Consistent with the Nr4a1 mRNA changes, Nr4a1 protein levels in hippocampal cultures were reduced by AP5 (100 μM, 24 hr) (Figure 1C, lane 2; quantified in Figure 1D). Conversely, Nr4a1 protein was induced by PTX (100 μM, 6 hr) and by a "chemical LTP" (cLTP) protocol (Forskolin + Rolipram [50 μM, 0.1 μM, 1 hr]) (Figures 1C and 1D), but it was suppressed by a chemical LTD (cLTD) protocol using bath application of NMDA (70 μM, 1 hr) (Figures 1C and 1D).

Time course experiments showed that both the 75 kDa and 85 kDa Nr4a1 bands were induced by 20 min after the start of PTX treatment and continued to rise over the next ~4 hr (up to about 4-fold) before falling back to baseline by ~10 hr (Figure 1E; quantified in Figure 1F). This induction by PTX was largely blocked by AP5, indicating that activity-dependent induction of Nr4a1 requires NMDARs (Figures 1G and 1H). In summary, Nr4a1 expression in neurons is bidirectionally controlled by synaptic NMDAR activity at both mRNA and protein levels.

Nr4a1 Transcriptional Activity Leads to Spine Loss

To explore Nr4a1 function, we first tested the effects of Nr4a1 overexpression in rat organotypic hippocampal slice cultures. Control CA1 pyramidal neurons transfected with GFP alone had spine density comparable to other reports (Hsieh et al., 2006; Shankar et al., 2007) (secondary apical dendrites, 6.63 ± 0.50/10 μm; basal dendrites, 5.09 ± 0.45/10 μm) (Figures 2A and 2B). In CA1 neurons overexpressing Nr4a1 plus GFP for 3–4 days, spine density was reduced by ~50% in both secondary apical dendrites (3.16 ± 0.67/10 μm, $p < 0.01$) and basal dendrites (2.58 ± 0.53/10 μm, $p < 0.01$) (Figures 2A and 2B). Overexpression of Nr4a1 for 6–8 days resulted in loss of the majority of spines (apical, ~80% loss, $p < 0.001$; basal, ~90% loss, $p < 0.001$) (Figures 2C and 2D). Notably, this did not alter the typical pyramidal cell shape or dendrite branching pattern (Figure 2C).

We also tested the effect of Nr4a1 overexpression in vivo. Cortical neurons of rat embryos were transfected by in utero electroporation at embryonic day 16 (E16) with DsRed plus or minus Nr4a1 expression plasmid. At 2.5–3 weeks after birth, neuronal morphology of layer 2/3 pyramidal neurons of somatosensory cortex was examined. In control neurons expressing DsRed only, spine density on secondary apical dendrites was 7.29 ± 0.30/10 μm (Figures 2E and 2F). In neurons cotransfected with Nr4a1 in addition to DsRed, the spine density was reduced by ~50% (3.69 ± 0.45/10 μm, $p < 0.001$) (Figures 2E and 2F), with no apparent change in dendrite branching (Figure 2E). These data show that Nr4a1 overexpression also eliminates spines in vivo.

Nr4a1 contains three typical nuclear receptor domains: an N-terminal transcription activation domain (TAD), a DNA-binding domain (DBD), and a C-terminal putative ligand-binding domain

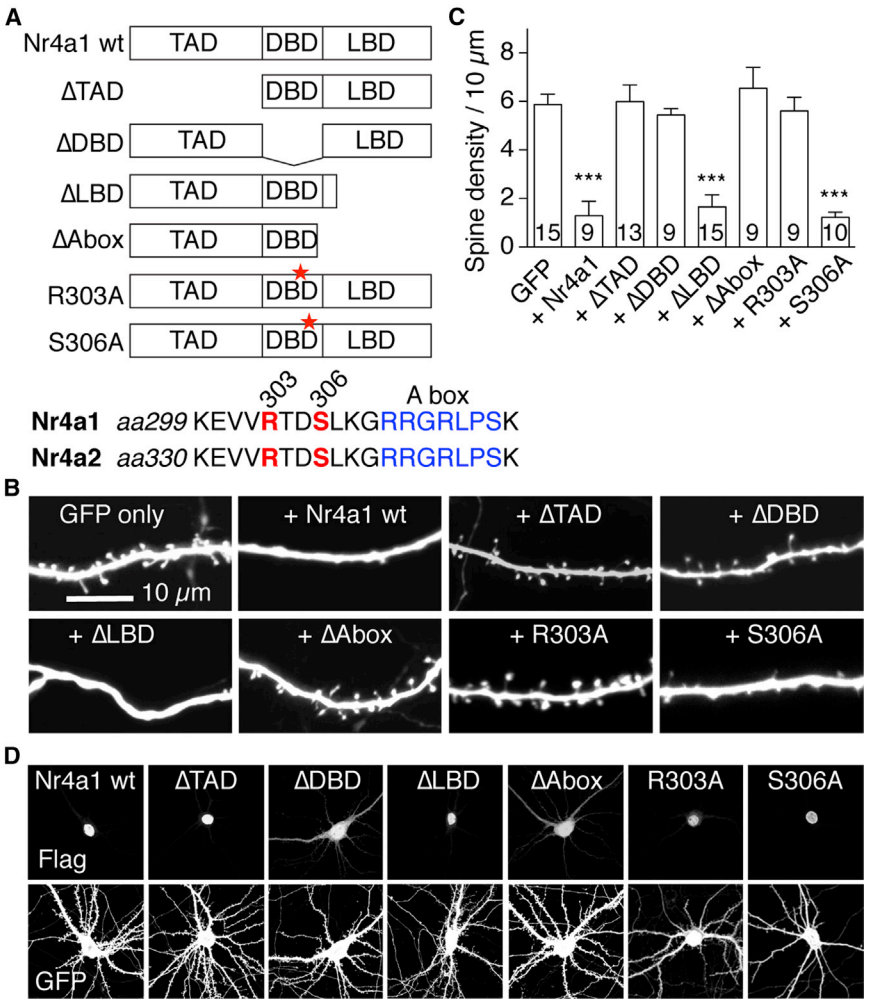

Figure 3. Transcriptional Activity Is Required for Nr4a1 to Eliminate Spines

(A) Top, schematic diagram of Nr4a1 domains and mutants. Bottom, amino acid sequence alignment of Nr4a2 and Nr4a1 showing the positions of the R303A and S306A point mutations (in red) and the "A box" (in blue).

(B) Sample images of basal dendrites from live CA1 pyramidal neurons transfected with GFP alone or cotransfected with indicated Nr4a1 mutants for 6–8 days.

(C) Quantitation of spine density in neurons transfected with indicated Nr4a1 mutants, compared with GFP alone. Number of neurons measured for each condition is indicated in the individual bars. Error bars show SEM. One-way ANOVA with Dunnett's multiple comparison test; ***$p < 0.001$.

(D) N-terminally Flag-tagged Nr4a1 and its mutants were cotransfected with GFP in neuronal cultures and stained for Flag (upper panels) and GFP (bottom panels).

(LBD) (Figure 3A). We made three deletion mutants, one for each domain, and tested the effects of these mutants on spine density. Mutants lacking the TAD (ΔTAD) or the DBD (ΔDBD) had no effect on spine density after 6–8 days overexpression, whereas the LBD deletion mutant (ΔLBD) was as effective as the wild-type Nr4a1 at reducing spine density Figures 3B and 3C). It has been reported that Nr4a family proteins do not require the LBD for their transcriptional activity (Wang et al., 2003). These results indicate that DNA binding and transcriptional activity of Nr4a1 are required for its ability to suppress spines.

The C-terminal end of the DBD contains a seven residue Abox that is responsible for recognizing the two adenine-thymidine base pairs at the 5′ end of the Nr4a1 DNA binding element (Wilson et al., 1992) (Figure 3A, in blue). Overexpression of a ΔAbox mutant, which lacks 11 more residues from the C-terminal end of ΔLBD, including the Abox (Figure 3A), had no effect on spine density (Figures 3B and 3C). This is consistent with the phenotype of the ΔDBD mutant and reaffirms the importance of DNA binding in suppression of spines by Nr4a1.

It has been reported that amino acid substitution R336A in the DBD of Nr4a2 abolishes its transcriptional activity, while a nearby mutation S339A is deficient in DNA damage repair but retains transcriptional activity (Malewicz et al., 2011). Nr4a1 and Nr4a2 are identical in this region (Figure 3A, bottom). We made the equivalent mutations in Nr4a1 and tested their effects on spine density: the transcriptional-deficient mutant R303A lost the efficacy to eliminate spines, whereas the S306A mutant with intact transcriptional activity removed spines similarly to wild-type (Figures 3B and 3C). This supports the conclusion that transcriptional activity of Nr4a1 is required for spine elimination.

All of the Flag-tagged Nr4a1 mutants expressed at similar levels in dissociated neurons, as measured by immunostaining for Flag (Figure 3D). Most of the mutants, with the exception of ΔDBD and ΔAbox, localized specifically in the nucleus like wild-type Nr4a1 (Figure 3D). The broader distribution of ΔDBD and ΔAbox is consistent with loss of a nuclear localization signal in the C-terminal end of the DBD (Katagiri et al., 2000).

Nr4a1 Overexpression Does Not Reduce Excitatory Synaptic Transmission

Spine density has been shown to generally correlate with excitatory synaptic strength, so we tested whether Nr4a1-mediated spine elimination also affected basal synaptic transmission. Simultaneous dual whole-cell patch-clamp recording was performed in hippocampal slice cultures on biolistically transfected CA1 pyramidal neurons and neighboring untransfected neurons (Futai et al., 2007). Schaffer collateral axons were stimulated to evoke synaptic responses. Surprisingly, the amplitude of evoked AMPAR-mediated EPSCs from neurons overexpressing Nr4a1 for 3–4 days (Figures 4A and 4B) or for 6–8 days (Figures S1A and S1B available online) was not significantly different from their nontransfected neighbors, despite

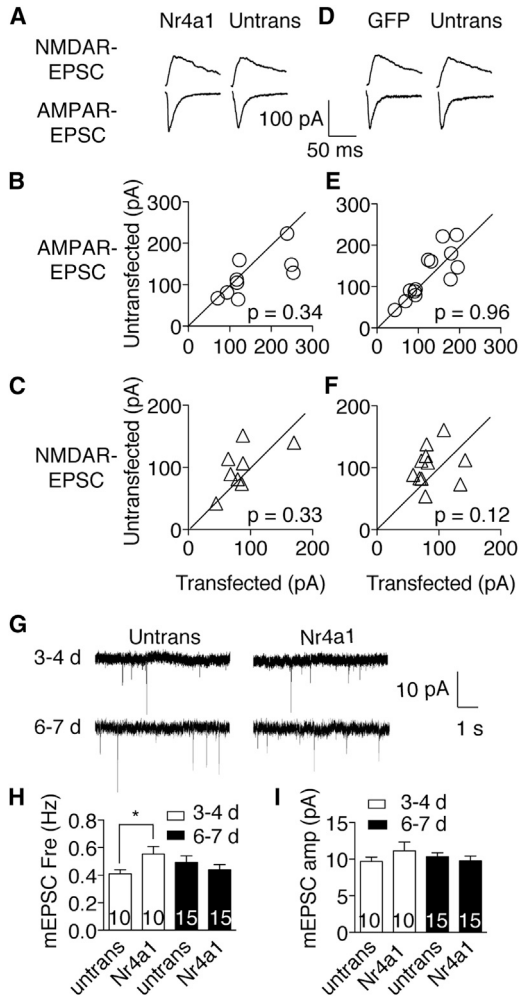

Figure 4. Nr4a1 Overexpression Does Not Reduce Excitatory Synaptic Transmission

Effect of expression of Nr4a1 plus GFP ([A]–[C]) or GFP alone ([D]–[F]) on excitatory synaptic transmission in hippocampal CA1 pyramidal cells in organotypic slice cultures. Expression vector for Nr4a1 was transfected together with pGFP-CAGGS at a ratio of 9:1 by weight. Neurons were recorded 3–4 days after transfection.

(A and D) Sample EPSC traces mediated by the AMPAR (downward) or NMDAR (upward) from pairs of transfected neurons (Nr4a1 or GFP) and neighboring untransfected neurons (untransfected). Stimulus artifacts were truncated.

(B, C, E, and F) EPSC amplitude are plotted for individual pairs of transfected and neighboring untransfected cells (open symbols). A total of 9 to 12 pairs of neurons were measured each condition.

(G) Representative traces of mEPSCs recorded from CA1 neurons in slice cultures transfected for 3–4 days or 6–7 days (as indicated) with Nr4a1 plus GFP and neighboring untransfected CA1 pyramidal neurons.

(H and I) Quantitation of frequency and amplitude of mEPSCs from experiments in (G). Mann-Whitney test for evoked EPSCs; p values shown in each graph ([B], [C], [E], and [F]). Student's t test for mEPSCs ([H] and [I]). Error bars show SEM. *p < 0.05. Number of neurons measured for each condition is indicated in the individual bars.

the fact that their spine density was much lower (Figure 2). Evoked NMDAR mediated EPSCs were also not altered (Figures 4A and 4C). GFP expression alone had no significant effect on AMPAR or NMDAR EPSCs, as expected (Figures 4D–4F, S1C, and S1D).

A small increase in mEPSC frequency, but not in mEPSC amplitude, was detected in neurons after 3–4 days of Nr4a1 overexpression (untransfected: 0.41 ± 0.03 Hz, transfected: 0.55 ± 0.05 Hz; p = 0.03) (Figures 4G–4I). In neurons transfected for 6–8 days with Nr4a1, which showed ~80% loss of spines, we found unaltered frequency and amplitude of mEPSCs compared with neighboring untransfected neurons (Figures 4G–4I).

Neither the amplitude nor the frequency of mIPSCs from neurons overexpressing Nr4a1 for 6–8 days was significantly different from their nontransfected neighbors (Figures S1E–S1G), indicating that Nr4a1 overexpression does not affect inhibitory synaptic transmission.

PSDs Are Localized on Dendritic Shaft in Nr4a1-Overexpressing Neurons

The unexpected finding that Nr4a1 overexpressing neurons had greatly reduced spine density but essentially normal excitatory synaptic transmission gave rise to the following question: where are the excitatory synapses localized? We tracked the position of excitatory synapses by coexpressing GFP-tagged PSD-95, a PSD scaffold protein (Kim and Sheng, 2004; Sheng and Hoogenraad, 2007). In control CA1 pyramidal neurons, as expected, the majority of PSD-95-GFP puncta (~72%) were found in the spine heads (red arrow, Figure 5A, quantified in 5D). In addition, there was weaker, diffuse PSD-95-GFP signal present in the dendritic shaft (Figure 5A). A minority of PSD-95-GFP puncta (~28%) appeared to be on the dendritic shaft ("shaft PSD," defined as a PSD-95-GFP punctum with >50% of its pixels overlapping with the dendritic shaft) (Figures 5A and 5D, yellow arrow). In neurons overexpressing Nr4a1 for 6–8 days, however, the great majority (~92%) of the PSD-95-GFP puncta were shaft PSDs (Figures 5B and 5D). Neurons overexpressing the mutant Nr4a1-R303A showed no change in the localization pattern of PSD-95-GFP puncta, which remained at spine heads predominantly (Figures 5C and 5D). Importantly, the total density of PSD-95-GFP puncta (Figure 5D) was not significantly altered by Nr4a1 expression. We also measured surface GluA1 levels by immunostaining and found that surface GluA1 immunofluorescence intensity per dendritic area was not altered by Nr4a1 expression compared with neurons expressing β-gal only (Figures 5E and 5F). These data indicate no change in density of excitatory synapses or surface AMPA receptor expression, consistent with lack of effect of Nr4a1 on excitatory synaptic transmission (Figure 4).

Nr4a1 Coordinately Regulates Plk2 and Rac1/RhoA Signaling Pathways Leading toward Spine Loss

We reasoned that Nr4a1 suppresses spines through its ability to alter gene transcription, since this morphological effect requires its transcriptional activity (Figure 3). To identify Nr4a1 regulated genes, we performed mRNA expression profiling by microarray on dissociated neuronal cultures infected with lentivirus encoding Nr4a1. Efficiency of infection with lentiviral vectors encoding Flag-tagged Nr4a1 or GFP was tested by immunostaining. At 6 days after infection, about 80% of the neurons in culture expressed GFP or Flag-Nr4a1 (Figures S2A and S2B): GFP had diffuse distribution throughout the neuron (Figure S2A), whereas

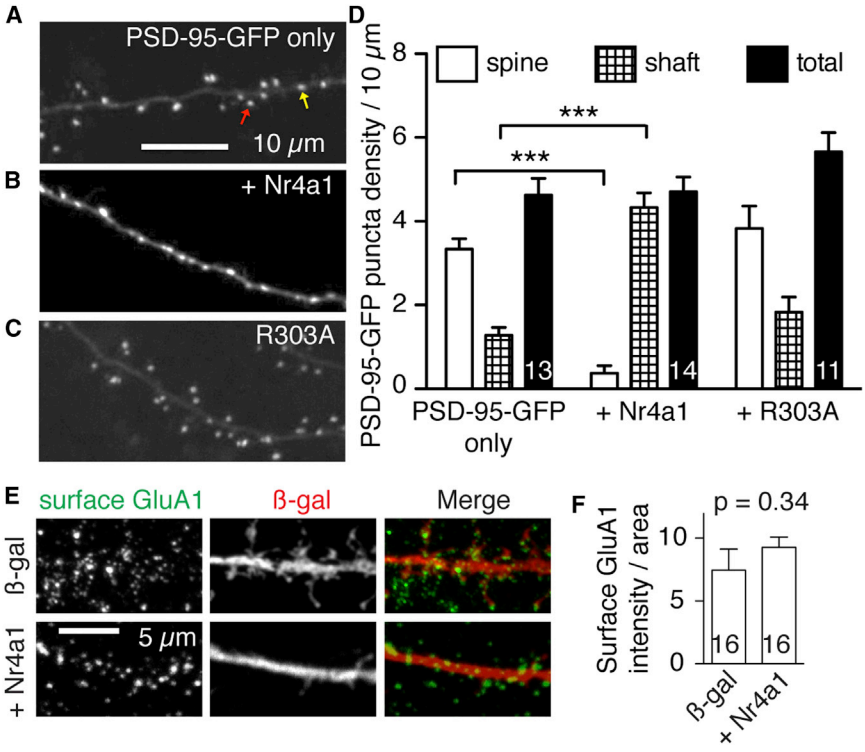

Figure 5. Excitatory PSDs and Surface GluA1 in Nr4a1-Expressing Neurons

(A, B, and C) sample images of dendrites transfected with PSD-95-GFP alone or cotransfected with PSD-95-GFP plus Nr4a1 or Nr4a1_R303A. Red arrow indicates PSD-95-GFP punctum located on spine; yellow arrow indicates a shaft PSD-95-GFP punctum.

(D) Quantitation of density of PSD-95-GFP puncta localized on spines, on shaft, or in total, measured from basal dendrites of CA1 pyramidal cells, transfected as indicated.

(E) Surface GluA1 staining from dissociated neurons transfected with Nr4a1 plus β-gal, or β-gal alone, for 6–8 days.

(F) Quantitation of surface GluA1 immunofluorescence intensity per square area of dendrite from experiments shown in (E). Error bars show SEM. Student's t test; ***$p < 0.001$. Number of neurons measured for each condition is indicated in the individual bars.

Flag-Nr4a1 was concentrated in nuclei, colocalized with DAPI staining (Figure S2B).

Clustering analysis of the microarray data showed a segregation of samples infected by the virus encoding GFP or Nr4a1, with Nr4a1 causing consistent mRNA expression changes in independent samples (Figure 6A). A total of 546 and 452 genes were significantly upregulated or downregulated, respectively, by Nr4a1 expression in dissociated hippocampal neuronal cultures ($log_2FC > 0.5$ or < -0.5; p value < 0.05) (Table S1). Gene ontology analysis highlighted that genes associated with the cytoskeleton were enriched (p value = 2.0×10^{-7}) in this limited set of upregulated and downregulated genes. Additionally, a gene-set-based approach performed using the entire expression array data set highlighted that genes annotated with the term "actin reorganization" were significantly downregulated after Nr4a1 treatment (p value = 3.0×10^{-2}). F-actin is a major cytoskeletal component of dendritic spines, and its reorganization is crucial for morphological changes of spines.

RhoA and Rac1 signaling pathways play major roles in the regulation of F-actin polymerization. Interestingly, Nr4a1 downregulated a RacGEF T cell lymphoma invasion and metastasis 2 (Tiam2) and two Rac1 downstream kinases, p21 protein (Cdc42/Rac)-activated kinase 1 (PAK1) and LIM domain kinase 1 (Limk1), whereas it upregulated a RhoA activator Rho guanine nucleotide exchange factor 11 (ARHGEF11) (Figure 6B). Given that F-actin is the main cytoskeletal component of dendritic spines, modulation of Rac1 and RhoA regulatory pathways could contribute to the spine morphology phenotypes we observed. We also identified two more Nr4a1-upregulated genes relevant to actin regulation, a RhoA activator Rhophilin-2 (Rhpn2) (Peck et al., 2002) and Plk2 (Figure 6B).

Rac1 and RhoA pathways have largely opposing roles in spine regulation (Govek et al., 2005; Saneyoshi et al., 2010). Rac1 promotes spine formation by enhancing actin polymerization via PAK1/3 and Limk1, whereas RhoA inhibits spine formation (Saneyoshi et al., 2010). Plk2 is an activity-induced negative regulator of spines and synapses (Pak and Sheng, 2003; Seeburg et al., 2008). The Nr4a1-induced elevation of ARHGEF11, Rhpn2, and Plk2 mRNAs and decrease of PAK1 and Limk1 mRNAs were verified by qRT-PCR (Figure 6C). Nr4a1 did not alter expression of RhoA, Rho-associated kinase 1 (Rock1) and Rac1 by either the microarray or qRT-PCR measurement (Figure 6C; Table S1). In summary, the downregulation of Tiam2, PAK1/3, and LimK1 mRNAs and the upregulation of ARHGEF11, Rhpn2, and Plk2 mRNAs by Nr4a1 would all be predicted to disfavor actin polymerization and perhaps in this way reduce spine density.

To test whether Nr4a1 actually regulates the actin cytoskeleton, we transfected GFP-tagged β-actin (GFP-ActB) in neurons. As expected, in control conditions, GFP-ActB was concentrated in puncta (spine heads) along the dendrites of CA1 pyramidal neurons (5.67 ± 0.36/10 μm) (Figure 6D; quantitation in Figure 6E). Nr4a1 coexpression reduced GFP-ActB puncta density by ~70% ($p < 0.0001$) (Figures 6D and 6E), and the remaining GFP-ActB clusters were localized on the dendritic shaft (Figure 6D). Thus, Nr4a1 overexpression in neurons resulted in disassembly of postsynaptic F-actin clusters, concomitant with loss of spines. However, simple disassembly of F-actin by itself seems not sufficient to explain the effect of Nr4a1 overexpression, because the actin depolymerizing drug Latrunculin A (5 μM concentration, 20 min) profoundly disrupted F-actin clusters yet had no significant effect on the density of PSD-95-GFP clusters or their predominant localization in spines (Figures S2C–S2E) (Allison et al., 2000; Kim and Lisman, 1999; Zito et al., 2004). Thus, the precise actin regulatory mechanisms that mediate spine loss by Nr4a1 remain unclear.

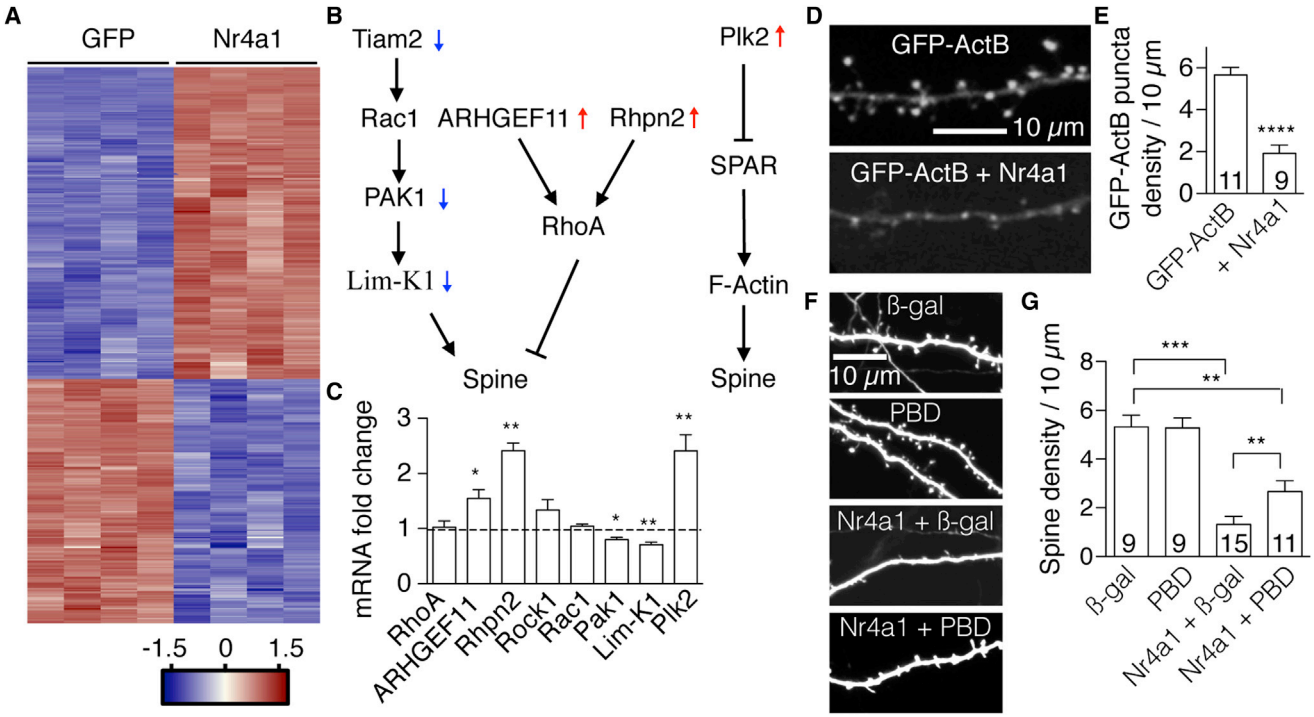

Figure 6. Nr4a1 Regulates Multiple mRNAs and Reduces F-Actin Puncta Density in Dendrites

(A) Clustering analysis of whole-genome mRNA profiling results comparing neuronal cultures infected with lentivirus-Nr4a1 versus lentivirus-GFP. A total of 546 upregulated and 452 downregulated genes are presented in the heat map ($log_2FC > 0.5$ or < -0.5; p value < 0.05).

(B) Simplified schematic of Rac1, RhoA, and Plk2 pathways and the regulation of pathway components by Nr4a1 overexpression. Tiam2, Pak1, and LimK1 are downregulated by Nr4a1 (blue arrows), while ARHGEF11, Rhpn2 and Plk2 are upregulated (red arrows).

(C) qRT-PCR measurement of mRNA changes induced by lentivirus-Nr4a1 (fold changes normalized to lentivirus-GFP infected controls).

(D) Representative images of dendrites of CA1 pyramidal neurons transfected with GFP-ActB alone or cotransfected with GFP-ActB plus Nr4a1.

(E) Quantitation of GFP-ActB puncta density from experiments shown in (D).

(F and G) Representative dendrites and their spine density quantitation from CA1 pyramidal neurons transfected with Nr4a1, PBD of Plk2, and/or β-gal, as indicated. (β-gal was used to equalize the total quantity of plasmids for each transfection condition.) Error bars show SEM. Student's t test; *p < 0.05; **p < 0.01; ***p < 0.001; ****p < 0.0001. Number of neurons measured for each condition is indicated in the individual bars.

For additional molecular manipulation, we focused on Plk2, because its mRNA/protein is normally expressed at low levels and highly induced by activity (Pak and Sheng, 2003). We tested whether the induction of Plk2 might contribute mechanistically to the spine elimination effect of Nr4a1. Under basal conditions, expression of β-gal or a dominant-negative construct of Plk2 (Polo box domain [PBD]) (Seeburg et al., 2008) by itself did not alter spine density in CA1 pyramidal cells of slice cultures (Figures 6F and 6G). Coexpression of Nr4a1 and β-gal with GFP dramatically reduced spine density ($p < 0.001$) (Figures 6F and 6G). Coexpression of PBD and Nr4a1 with GFP, however, significantly blunted the loss of spine density induced by Nr4a1 ($p < 0.01$) (Figures 6F and 6G), suggesting that Plk2 function may contribute to the spine elimination phenotype of Nr4a1 overexpression. However, the incomplete reversal by PBD may imply Plk2 is not solely responsible for the Nr4a1-induced spine loss.

Nr4a1 Knockdown Results in Clustered Spines, PSDs, and F-Actin at the Distal Ends of Dendrites

To understand the physiological function of Nr4a1, we designed two shRNA constructs to knock down endogenous Nr4a1. Compared with a control shRNA against firefly luciferase (shLuc), two distinct Nr4a1 shRNAs (shNr4a1_1, shNr4a1_2) were found to suppress the expression of Flag-tagged Nr4a1 protein, but not Flag-tagged Nr4a2 and Nr4a3, in HEK293 cells (Figure S3A). In dissociated hippocampal cultures, transfection of shNr4a1_1 or shNr4a1_2, but not shLuc, reduced PTX-induced Nr4a1 staining in the nuclei of transfected neurons (Figure S3B). The diffuse cytoplasmic staining detected by Nr4a1 antibody remained after shNr4a1 transfection, suggesting it is nonspecific background. The nuclear localization of Nr4a1 is consistent with its role as a nuclear receptor.

Although overexpression of Nr4a1 strongly reduced spine density in hippocampal slice cultures (Figure 2), shRNA knockdown of Nr4a1 had no significant effect on spine density of CA1 pyramidal cells (Figures S3C and S3D). A possible explanation for the lack of effect is the low basal expression of Nr4a1 in hippocampal slice cultures (Figures 1B and 1C).

Before investigating the role of activity-induced Nr4a1, we characterized the time course of induction of Nr4a1 in organotypic slice cultures by PTX. Elevation of Nr4a1 mRNA occurred by 1 hr after start of PTX treatment (~8 fold increase), and was

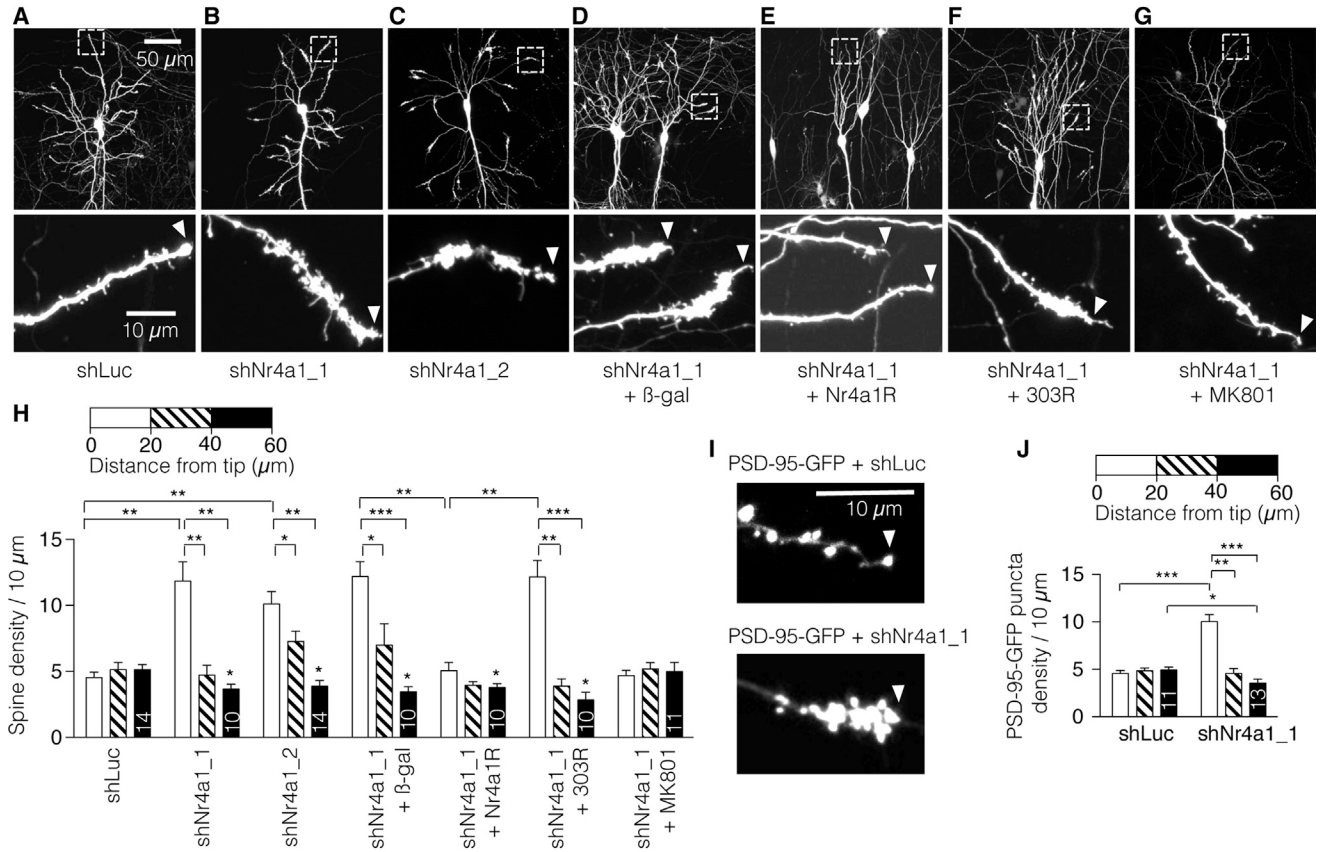

Figure 7. Nr4a1 Knockdown in Chronically Hyperactive Neurons Results in Increased Density of Spines and PSD-95-GFP Puncta at Dendrite Tips in an NMDAR-Dependent Manner

(A–G) Representative dendrites and CA1 pyramidal neurons transfected with GFP plus different shRNAs and shRNA-resistant Nr4a1 construct (Nr4a1R), as indicated, imaged after 48 hr PTX treatment. Cultures were coincubated with MK801 in (G). Boxed region is shown at higher magnification in lower panels. White arrowheads indicate the distal tip of dendrite.

(H) Quantitation of spine density (binned in 20 μm segments from the tip) in basal dendrites of CA1 neurons from experiment shown in (A)–(G).

(I) Representative images of PSD-95-GFP puncta from CA1 pyramidal neurons expressing shLuc control (top) or shNr4a1_1 (bottom), after 48 hr PTX treatment. White arrowheads indicate tip of dendrite.

(J) PSD-95-GFP puncta density quantitation in 20 μm bins from the distal tips of secondary basal dendrites. Error bars show SEM. Student's t test; *p < 0.05; **p < 0.01; ***p < 0.001. Number of neurons measured for each condition is indicated in the individual bars.

sustained for more than 24 hr, before returning back to baseline after 2 days (Figure S3E). Compared to Nr4a1, Nr4a3 mRNA showed a slower and more moderate increase (Figure S3E).

To test the function of activity-induced Nr4a1 in spine regulation, we transfected hippocampal slice cultures with Nr4a1 shRNAs plus GFP and then treated the slices with PTX for 1–2 days before imaging. Remarkably, in these chronically hyperactive slice cultures, we observed massive clustering of spines at the distal ends of both apical and basal dendrites in the neurons transfected with either of the Nr4a1 shRNAs, such that the dendrite ends took on a "tube brush" appearance (Figures 7A–7C; distal tips of dendrites are indicated by white arrowheads). Quantitation showed that in the control (shLuc) neurons, spines were relatively evenly distributed along the dendrites in the distal to proximal axis (Figure 7H, binned in 20 μm segments from the tip of the secondary dendrites). In neurons transfected with either Nr4a1 shRNA shNr4a1_1 or shNr4a1_2, however, spine density was much higher at the distal ends of dendrites (0–20 μm from dendrite tip) but were comparable to shLuc-expressing neurons in the more proximal regions (20–40 μm from dendrite tip) (Figure 7H). A small reduction in spine density was detected in the most proximal region measured (40–60 μm from dendrite tip) (Figure 7H). The abnormal increase of spine density at the distal ends of dendrites was prevented by coexpression of an shRNA-resistant Nr4a1 cDNA expressing wild-type Nr4a1 (Nr4a1R), but not by coexpression of β-gal or the Nr4a1_R303A mutant (303R) with deficient transcriptional activity (Figures 7D–7F and 7H). These data indicate that the effect of Nr4a1 shRNAs on distal-dendrite spine density is likely to be specifically caused by Nr4a1 knockdown, rather than a nonspecific effect of shRNA. Moreover, the PTX-induced spine clustering in Nr4a1 knockdown neurons was completely blocked by NMDAR antagonist MK-801 (50 μM), suggesting NMDAR activity is required to drive this distal spine accumulation (Figures 7G and 7H).

Since spines are usually the sites of excitatory synapses, we asked whether excitatory synapses are also distributed to the

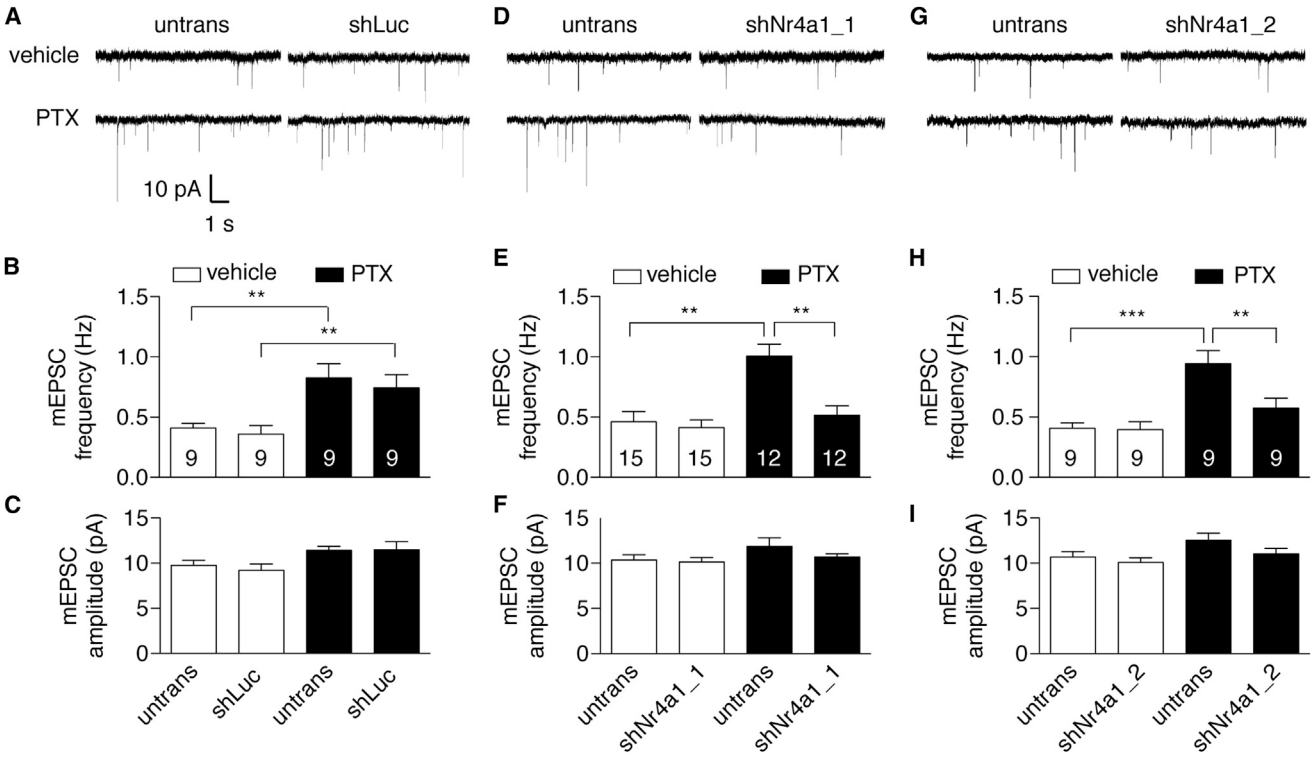

Figure 8. Knockdown of Nr4a1 Impairs Synaptic Potentiation Induced by Chronic Hyperactivity

(A, D, and G) Representative traces of mEPSCs recorded from CA1 pyramidal neurons expressing luciferase shRNA (shLuc) (A) or Nr4a1 shRNA ([D]: shNr4a1_1; [G]: shNr4a1_2), compared with their neighboring untransfected neurons from organotypic slice cultures treated for 2 days with vehicle (top) or PTX (bottom). (B, C–F, and H) Quantitation of mEPSC frequencies and amplitude measured from neurons expressing shLuc ([B] and [C]), shNr4a1_1 ([E] and [F]), or shNr4a1_2 ([H] and [I]) compared with their neighboring untransfected neurons. Error bars show SEM. Student's t test; $^{**}p < 0.01$; $^{***}p < 0.001$. Number of neurons measured for each condition is indicated in the individual bars.

distal ends of dendrites by Nr4a1 knockdown in PTX-treated neurons of hippocampal slice cultures. To address this question, we used PSD-95-GFP as a marker to visualize PSDs of excitatory synapses. In unstimulated (vehicle-treated) neurons, PSD-95-GFP puncta distributed evenly along the secondary dendrites, regardless of transfection of shLuc or shNr4a1_1 (Figures S3F and S3G) (PSD-95-GFP puncta density measured in 20 μm bins from the tip of the secondary dendrites). Two days of PTX treatment did not alter PSD-95-GFP puncta distribution pattern in the neurons expressing shLuc (Figure 7I, upper) but caused a marked accumulation of PSD-95-GFP puncta at the distal ends of dendrites in shNr4a1_1-transfected neurons (Figure 7I, bottom). Neurons transfected with shNr4a1_1 had ~2-fold more PSD-95-GFP puncta at the dendrite tips compared with shLuc-expressing neurons (Figure 7J). Consistent with the spine density results, PSD-95-GFP puncta density in the more proximal region (20–40 μm from dendrite tip) was comparable between shNr4a1_1 and control, and there was a small reduction of puncta density in the region of 40–60 μm from the dendrite tip in neurons expressing shNr4a1_1 (Figure 7J). The PSD-95-GFP clusters that accumulated at the distal ends of dendrites appeared to be bona fide synapses in that a high percentage of them show overlap or apposition with presynaptic marker synapsin I puncta, similar to PSD-95-GFP clusters in control neurons (~70%; Figure S4).

As with PSD-95 puncta, 48 hr PTX treatment also caused distal accumulation of GFP-ActB puncta in ~60% of the neurons expressing shNr4a1_1 but not in any of the neurons expressing shLuc (Figure S5A). Compared with PSD-95-GFP puncta that showed clearer segregation, GFP-ActB signals overlapped extensively with each other at the distal ends of PTX-treated shNr4a1_1 transfected neurons, making it impossible to count puncta density (Figure S5A, bottom). Together, these data reveal a redistribution of spines, excitatory synapses, and F-actin puncta to the distal ends of dendrites in neurons deficient in Nr4a1 during prolonged hyperactivity.

Loss of Nr4a1 Impairs Synaptic Potentiation Induced by Chronic Hyperactivity in Hippocampal Slice Cultures

To evaluate the impact of Nr4a1 knockdown on excitatory synaptic transmission, we measured mEPSCs from CA1 pyramidal neurons transfected with Nr4a1 shRNAs or shLuc as well as their neighboring untransfected neurons (Figure 8). Neither Nr4a1 shRNAs (shNr4a1_1 and shNr4a1_2) nor shLuc control altered amplitude or frequency of mEPSCs in CA1 pyramidal cells compared with their neighboring untransfected neurons under basal conditions (vehicle treatment) (Figure 8). Following PTX treatment of hippocampal slice cultures (100 μM, 48 hr), mEPSC frequency increased in CA1 pyramidal neurons by ~2-fold, comparable to previous reports showing that elevating activity by

blocking $GABA_A$Rs enhances excitatory synaptic transmission in hippocampal slice cultures (Abegg et al., 2004; Seeburg and Sheng, 2008). Expression of shLuc had no effect on basal mEPSC frequency and did not affect the enhancement of mEPSC frequency by PTX (Figures 8A and 8B). Knockdown of Nr4a1 by either shNr4a1_1 or shNr4a1_2 had no effect on basal mEPSC frequency but significantly reduced mEPSC frequency in PTX-treated slices, compared with untransfected neighboring neurons (Figures 8D, 8E, 8G, and 8H). There was a trend of increasing mEPSC amplitudes in PTX-treated neurons, but this did not reach statistical significance (Figures 8C, 8F, and 8I). Overall, these results show that Nr4a1 expression—which is induced by PTX—is required for the normal synaptic potentiation by PTX in this experimental preparation. Our findings affirm a role for Nr4a1 in activity-dependent synaptic plasticity and are in line with a previous report that dominant-negative Nr4a1 transgenic mice have deficits in L-LTP and learning and memory with normal basal synaptic transmission (Bridi and Abel, 2013; Hawk et al., 2012).

Nr4a1 Knockdown Results in Enhanced Spine Density at the Distal Ends of Dendrites In Vivo

What is the effect of Nr4a1 knockdown in vivo? Rat cortical neurons were transfected by in utero electroporation at E16 with shLuc or shNr4a1_1 plus DsRed as a transfection marker and cell fill. Examined at 2.5–3 weeks after birth, in neurons transfected with shNr4a1_1, spine density at the distal ends of dendrites (0–20 and 20–40 μm from distal ends) was significantly higher than control neurons transfected with shLuc (0–20 μm: shNr4a1_1: 7.86 ± 0.52/10 μm; shLuc: 5.49 ± 0.56/10 μm; $p < 0.01$; 20–40 μm: shNr4a1_1: 7.82 ± 0.42/10 μm; shLuc: 6.22 ± 0.44/10 μm; $p < 0.01$) (Figures S5B, S5C, and S5D). In more proximal regions of secondary dendrites (40–60 μm from tip), the spine density of shNr4a1_1-expressing neurons was not different from shLuc-transfected neurons (shNr4a1_1: 7.54 ± 0.35/10 μm; shLuc: 7.92 ± 0.45/10 μm) (Figure S5B–S5D). Thus, Nr4a1 knockdown in vivo is sufficient to enhance spine density preferentially at the distal ends of dendrites.

DISCUSSION

Long-lasting synaptic plasticity requires NMDAR activity and gene expression, but the role of NMDAR-induced genes in regulation of synapse structure and function remains incompletely understood. In the present study, we show that an NMDAR-induced nuclear receptor, Nr4a1, regulates the density of spines and the distribution pattern of spines and excitatory synapses.

Nr4a1 Eliminates Dendritic Spines without Affecting Excitatory Synaptic Transmission

Overexpression of Nr4a1 eliminated the majority of spines on pyramidal neurons, but the strength of excitatory synaptic transmission was unaffected. The preservation of EPSC in spine-deficient neurons is associated with an increased fraction of PSDs localized on the dendritic shaft. This redistribution is consistent with previous studies showing that PSDs are dynamic structures that can move to the dendritic shafts at the sites of retracted spines (Woods et al., 2011). More importantly, like spineless interneurons, pyramidal neurons with predominantly shaft PSDs can maintain synaptic function. Thus, spine architecture seems dispensable for excitatory synaptic transmission in pyramidal neurons.

It has been long known that spines are the primary loci for excitatory inputs. Since Cajal's speculation that spines increase a dendrite's surface area, the fundamental importance of spines remains a debated question. Why do excitatory axons contact neurons on spines instead of dendritic shafts? Three main hypotheses have been proposed: (1) spines enhance synaptic connectivity, (2) spines function as electrical compartments to modify synaptic potentials, and (3) spines provide biochemical compartments to implement input-specific synaptic plasticity (Shepherd, 1996; Yuste, 2011). The first hypothesis predicts reduction of synaptic connectivity in the absence of spines. Our results argue against this idea, because excitatory synaptic transmission (including mEPSC amplitude and frequency) appears intact despite loss of ~80% of spines after Nr4a1 overexpression. However, our results do not exclude the possibility that spines could promote synaptic connectivity over a much longer period of time or during some specific developmental stage when synapses are more actively forming. With regard to the second and third hypotheses, our finding could provide an opportunity to test them in spineless pyramidal neurons.

Recent studies have shown that functional and structural synaptic plasticity can be dissociated (He et al., 2011; Pi et al., 2010; Wang et al., 2007). Additionally, using single-cell knockout of AMPARs or both AMPARs and NMDARs, Lu and colleagues showed that excitatory synaptic transmission can be abolished without altering pyramidal neuron dendritic branching or spine density, implying that spine structure does not depend on excitatory synaptic transmission (Lu et al., 2009, 2013). Our results are consistent with and complementary to these findings.

Nr4a1 Regulates Gene Transcription Leading toward Spine Loss

Spine number and morphology can be regulated through control of the actin cytoskeleton. Plk2—an activity-inducible kinase that plays a role in synaptic homeostasis—is believed to eliminate spines, at least in part, by promoting degradation of SPAR, a Rap GTPase activating protein that regulates F-actin and Rap signaling (Pak and Sheng, 2003; Pak et al., 2001; Seeburg et al., 2008). In addition to spine structure, Plk2 can also negatively regulate synaptic strength by a kinase-independent mechanism, through disrupting *N*-ethylmaleimide-sensitive fusion-protein-mediated stabilization of surface AMPARs (Evers et al., 2010). In our results, induction of Plk2 may contribute to the spine loss caused by Nr4a1 overexpression; however, the lack of effect of Nr4a1 on synaptic transmission argues against a major effect of Plk2 on AMPARs. Plk2 may be transcriptionally regulated by Nr4a1, as its promoter contains putative Nr4a response elements, and Plk2 expression is reduced in myeloid cells from *Nr4a1*$^{-/-}$ and *Nr4a3*$^{+/-}$ mice (Ramirez-Herrick et al., 2011).

Spine morphogenesis is controlled by Rac1 and RhoA in largely opposing fashion (Govek et al., 2005; Saneyoshi et al., 2010). Rac1 signaling promotes actin polymerization, and inhibition of the Rac1 pathway decreases spine density. Conversely, activation of the RhoA pathway decreases spine density (Govek et al., 2005; Nakayama et al., 2000; Saneyoshi et al., 2010;

Tashiro and Yuste, 2004). We find that Nr4a1 increases expression of the RhoA positive regulators, Rhpn2 and ARHGEF11, and reduces expression of the RacGEF, Tiam2 (Peck et al., 2002; Tolias et al., 2005), as well as two kinases downstream of Rac1, PAK1 and Limk1 (Saneyoshi et al., 2010). These changes would be predicted to enhance RhoA and reduce Rac1 signaling, which should favor spine loss. Overall, we suggest that modulation of Rac1, RhoA, and Plk2 pathways by Nr4a1 contributes to the mechanism of Nr4a1-induced spine loss, but the downstream effectors of these pathways and the precise role of F-Actin in this process remain unclear. Nr4a1 also decreases the expression of Lrrtm2 and Lrrtm4 (Table S1), postsynaptic adhesion molecules that promote synapse formation through binding to presynaptic partners (Ko et al., 2011; Siddiqui et al., 2013). Whether these gene expression alterations contribute to the spine loss effect of Nr4a1 or not remains to be tested.

Endogenous Nr4a1 Prevents Abnormal Spines and PSDs Clustering at the Distal Ends of Dendrites

Normally in cortical pyramidal neurons, spines exhibit a nonuniform distribution pattern along primary and secondary dendrites. Spine density is lowest near the soma and increases gradually to a maximum at 40–100 μm from the soma but then decreases slightly at the most distal end of secondary dendrites in both human and rodent brains (Cheetham et al., 2008; Larkman, 1991; Marin-Padilla, 1967). The molecular mechanisms regulating the distal decrease of spine density are largely unknown. Our finding that knockdown of Nr4a1 shifts the distribution of excitatory synapses toward the distal ends of dendrites during chronic hyperactivity, but not under basal conditions, suggests that Nr4a1 functions as an activity-induced homeostatic mechanism to prevent distal accumulation of synapses/spines on dendrites, thereby maintaining the normal distribution pattern of spines. Nr4a1 shRNA only slightly increases distal spine density in vivo, perhaps because the in vivo state reflects an intermediate level of activity between chronic PTX-treated and untreated conditions in culture. Therefore activity-induced Nr4a1 provides the first molecular mechanism that controls synaptic density at the distal ends of dendrites.

As a function of distance from the cell body, different domains of dendrites display different electrical properties and functions, presumably based on protein expression gradients (Hoffman and Johnston, 1998; Magee, 2000). Certain proteins (such as Plk2, HCN1, and Kv4.2 A-type K+ channels) have been reported to show a gradient of protein level as a function of distance from the cell body (Hoffman and Johnston, 1998; Lörincz et al., 2002; Pak and Sheng, 2003). Plk2 accumulates preferentially in the more proximal region of dendrites (Pak and Sheng, 2003), whereas HCN1 and A-type K+ channels show higher density in the distal dendrite (Hoffman and Johnston, 1998; Lörincz et al., 2002). Plk2 is an Nr4a1-regulated gene; however, the increased density of PSD-95 puncta in distal dendrites seen with Nr4a1 knockdown cannot be simply explained by impaired induction of Plk2, because Plk2 promotes loss of PSDs, and the normal gradient of Plk2 should favor a higher density of PSDs in distal dendrites. Nonetheless, it is possible that Nr4a1-induced downstream effectors other than Plk2 could display a proximal-to-distal gradient and act to inhibit distal accumulation of PSDs.

When Nr4a1 induction is abrogated in conditions of chronic hyperactivity, the excessive clustering of spines/synapses and F-actin at distal ends of dendrites is associated with a defect in the potentiation of excitatory synaptic transmission, as measured by increased frequency of mEPSCs. It is unclear, however, whether the misdistribution of synapses is causally related to the synaptic deficits.

In summary, we show here that NMDAR-induced Nr4a1 is a transcriptional regulator of the actin cytoskeleton that adjusts spine/PSD density and distribution. Such activity-dependent control of synapses could be a mechanism by which Nr4a1 is involved in long-term memory and neuronal protection.

EXPERIMENTAL PROCEDURES

Additional details can be found in Supplemental Information.

Expression Vectors and Drugs

Flag-Nr4a1, EGFP (GFP), PSD-95-GFP, GFP-β-Actin (GFP-ActB), and mKate2-ActB (Evrogen) were subcloned into pCAGGS under control of a CAG promoter (chicken β-actin promoter with a CMV enhancer). shRNAs were all expressed by a pSuper vector. All drugs for this study were purchased from Sigma.

Neuronal Cultures and Lentiviral Infection

Embryonic rat and mouse hippocampal neuronal cultures were grown in B27 neurobasal medium. For lentiviral studies, Nr4A1 or GFP was subcloned into the FHSynGW backbone vector, which drives cDNA expression using a human Synapsin I promoter (Provided by Dr. Carlos Lois, MIT). Lentiviral particles were produced using the method described previously (Lois et al., 2002), and viral titer was estimated by serial dilution infections of HEK293 cells.

Western Blotting

Proteins were separated by 4%–20% Tris-glycine SDS-PAGE and transferred to nitrocellulose membranes (Life Technologies). Primary antibodies were applied in blocking buffer overnight at 4°C. The signal was detected using SuperSignal West Dura Chemiluminescent substrate (Thermo Scientific) with a Versadoc imaging system (Bio-Rad).

Organotypic Hippocampal Slice Culture, Transfection, Imaging, and Electrophysiology

Organotypic slice cultures were made from P7 Sprague-Dawley rats and were biolistically transfected with a gene gun (Biorad) at DIV3–DIV6. Transfected neurons were imaged live by a fluorescence confocal microscope or patch-clamp recorded 3–8 days after transfection. All transfections and imaging were performed and analyzed by investigators blinded to the conditions.

Rat Cortical In Utero Electroporation and Spine Imaging

L2/3 pyramidal neurons were fluorescently labeled by in utero transfection of progenitor cells with a CAGGs promoter-based expression plasmid containing the cDNA for the red fluorescent protein DsRed-Express (DsRed) at embryonic day 16. Individual dendrites and spines from PFA fixed brain sections were visualized by DsRed fluorescence using a confocal microscope.

Microarray mRNA Profiling

After 10 days in culture, dissociated mouse hippocampal neurons in 6-well plates were infected with lentivirus expressing either Flag-Nr4a1 or GFP and incubated for 6 days to allow for transgene expression. Total RNA was then isolated using RNeasy plus kit (QIAGEN). Samples passing an mRNA quality check proceeded to quantitative analysis on Agilent 4×44 Mouse Microarrays.

Statistical Analysis and Animal Policy

Statistical analyses are described in the Figure Legends.

All animal procedures were reviewed and approved by the Institutional Animal Care and Use Committee at Genentech and are in accordance with

the National Institutes of Health's *Guide for the Care and Use of Laboratory Animals*.

SUPPLEMENTAL INFORMATION

Supplemental Information includes five figures, one table, and Supplemental Experimental Procedures and can be found with this article online at http://dx.doi.org/10.1016/j.neuron.2014.05.027.

ACKNOWLEDGMENTS

We thank Drs. Yi Zuo (UC Santa Cruz) and Karen Zito (UC Davis) for their suggestions in experimental design and Drs. Christopher Nelson, Felix Yeh, Michael Chang, Qiang Zhou, Shih-Ching Lo, Zora Modrusan, and Robert Soriano (Genentech Inc.) for intellectual or technical input and manuscript editing.

Accepted: May 6, 2014
Published: June 26, 2014

REFERENCE

Abegg, M.H., Savic, N., Ehrengruber, M.U., McKinney, R.A., and Gähwiler, B.H. (2004). Epileptiform activity in rat hippocampus strengthens excitatory synapses. J. Physiol. *554*, 439–448.

Alberini, C.M. (2009). Transcription factors in long-term memory and synaptic plasticity. Physiol. Rev. *89*, 121–145.

Allison, D.W., Chervin, A.S., Gelfand, V.I., and Craig, A.M. (2000). Postsynaptic scaffolds of excitatory and inhibitory synapses in hippocampal neurons: maintenance of core components independent of actin filaments and microtubules. J. Neurosci. *20*, 4545–4554.

Barbosa, A.C., Kim, M.S., Ertunc, M., Adachi, M., Nelson, E.D., McAnally, J., Richardson, J.A., Kavalali, E.T., Monteggia, L.M., Bassel-Duby, R., and Olson, E.N. (2008). MEF2C, a transcription factor that facilitates learning and memory by negative regulation of synapse numbers and function. Proc. Natl. Acad. Sci. USA *105*, 9391–9396.

Barneda-Zahonero, B., Servitja, J.M., Badiola, N., Miñano-Molina, A.J., Fadó, R., Saura, C.A., and Rodríguez-Alvarez, J. (2012). Nurr1 protein is required for N-methyl-D-aspartic acid (NMDA) receptor-mediated neuronal survival. J. Biol. Chem. *287*, 11351–11362.

Benito, E., Valor, L.M., Jimenez-Minchan, M., Huber, W., and Barco, A. (2011). cAMP response element-binding protein is a primary hub of activity-driven neuronal gene expression. J. Neurosci. *31*, 18237–18250.

Bridi, M.S., and Abel, T. (2013). The NR4A orphan nuclear receptors mediate transcription-dependent hippocampal synaptic plasticity. Neurobiol. Learn. Mem. *105*, 151–158.

Cheetham, C.E., Hammond, M.S., McFarlane, R., and Finnerty, G.T. (2008). Altered sensory experience induces targeted rewiring of local excitatory connections in mature neocortex. J. Neurosci. *28*, 9249–9260.

Chen, D.Y., Bambah-Mukku, D., Pollonini, G., and Alberini, C.M. (2012). Glucocorticoid receptors recruit the CaMKIIα-BDNF-CREB pathways to mediate memory consolidation. Nat. Neurosci. *15*, 1707–1714.

El-Husseini, A.E., Schnell, E., Chetkovich, D.M., Nicoll, R.A., and Bredt, D.S. (2000). PSD-95 involvement in maturation of excitatory synapses. Science *290*, 1364–1368.

Evers, D.M., Matta, J.A., Hoe, H.S., Zarkowsky, D., Lee, S.H., Isaac, J.T., and Pak, D.T. (2010). Plk2 attachment to NSF induces homeostatic removal of GluA2 during chronic overexcitation. Nat. Neurosci. *13*, 1199–1207.

Flavell, S.W., Cowan, C.W., Kim, T.K., Greer, P.L., Lin, Y., Paradis, S., Griffith, E.C., Hu, L.S., Chen, C., and Greenberg, M.E. (2006). Activity-dependent regulation of MEF2 transcription factors suppresses excitatory synapse number. Science *311*, 1008–1012.

Flavell, S.W., Kim, T.K., Gray, J.M., Harmin, D.A., Hemberg, M., Hong, E.J., Markenscoff-Papadimitriou, E., Bear, D.M., and Greenberg, M.E. (2008). Genome-wide analysis of MEF2 transcriptional program reveals synaptic target genes and neuronal activity-dependent polyadenylation site selection. Neuron *60*, 1022–1038.

Futai, K., Kim, M.J., Hashikawa, T., Scheiffele, P., Sheng, M., and Hayashi, Y. (2007). Retrograde modulation of presynaptic release probability through signaling mediated by PSD-95-neuroligin. Nat. Neurosci. *10*, 186–195.

Govek, E.E., Newey, S.E., and Van Aelst, L. (2005). The role of the Rho GTPases in neuronal development. Genes Dev. *19*, 1–49.

Hawk, J.D., and Abel, T. (2011). The role of NR4A transcription factors in memory formation. Brain Res. Bull. *85*, 21–29.

Hawk, J.D., Bookout, A.L., Poplawski, S.G., Bridi, M., Rao, A.J., Sulewski, M.E., Kroener, B.T., Manglesdorf, D.J., and Abel, T. (2012). NR4A nuclear receptors support memory enhancement by histone deacetylase inhibitors. J. Clin. Invest. *122*, 3593–3602.

Hayashi, Y., and Majewska, A.K. (2005). Dendritic spine geometry: functional implication and regulation. Neuron *46*, 529–532.

Hazel, T.G., Misra, R., Davis, I.J., Greenberg, M.E., and Lau, L.F. (1991). Nur77 is differentially modified in PC12 cells upon membrane depolarization and growth factor treatment. Mol. Cell. Biol. *11*, 3239–3246.

He, K., Lee, A., Song, L., Kanold, P.O., and Lee, H.K. (2011). AMPA receptor subunit GluR1 (GluA1) serine-845 site is involved in synaptic depression but not in spine shrinkage associated with chemical long-term depression. J. Neurophysiol. *105*, 1897–1907.

Hoffman, D.A., and Johnston, D. (1998). Downregulation of transient K+ channels in dendrites of hippocampal CA1 pyramidal neurons by activation of PKA and PKC. J. Neurosci. *18*, 3521–3528.

Holtmaat, A., and Svoboda, K. (2009). Experience-dependent structural synaptic plasticity in the mammalian brain. Nat. Rev. Neurosci. *10*, 647–658.

Hsieh, H., Boehm, J., Sato, C., Iwatsubo, T., Tomita, T., Sisodia, S., and Malinow, R. (2006). AMPAR removal underlies Abeta-induced synaptic depression and dendritic spine loss. Neuron *52*, 831–843.

Katagiri, Y., Takeda, K., Yu, Z.X., Ferrans, V.J., Ozato, K., and Guroff, G. (2000). Modulation of retinoid signalling through NGF-induced nuclear export of NGFI-B. Nat. Cell Biol. *2*, 435–440.

Kim, C.H., and Lisman, J.E. (1999). A role of actin filament in synaptic transmission and long-term potentiation. J. Neurosci. *19*, 4314–4324.

Kim, E., and Sheng, M. (2004). PDZ domain proteins of synapses. Nat. Rev. Neurosci. *5*, 771–781.

Ko, J., Soler-Llavina, G.J., Fuccillo, M.V., Malenka, R.C., and Südhof, T.C. (2011). Neuroligins/LRRTMs prevent activity- and Ca2+/calmodulin-dependent synapse elimination in cultured neurons. J. Cell Biol. *194*, 323–334.

Kopec, C.D., Li, B., Wei, W., Boehm, J., and Malinow, R. (2006). Glutamate receptor exocytosis and spine enlargement during chemically induced long-term potentiation. J. Neurosci. *26*, 2000–2009.

Lang, C., Barco, A., Zablow, L., Kandel, E.R., Siegelbaum, S.A., and Zakharenko, S.S. (2004). Transient expansion of synaptically connected dendritic spines upon induction of hippocampal long-term potentiation. Proc. Natl. Acad. Sci. USA *101*, 16665–16670.

Larkman, A.U. (1991). Dendritic morphology of pyramidal neurones of the visual cortex of the rat: III. Spine distributions. J. Comp. Neurol. *306*, 332–343.

Lois, C., Hong, E.J., Pease, S., Brown, E.J., and Baltimore, D. (2002). Germline transmission and tissue-specific expression of transgenes delivered by lentiviral vectors. Science *295*, 868–872.

Lörincz, A., Notomi, T., Tamás, G., Shigemoto, R., and Nusser, Z. (2002). Polarized and compartment-dependent distribution of HCN1 in pyramidal cell dendrites. Nat. Neurosci. *5*, 1185–1193.

Lu, W., Shi, Y., Jackson, A.C., Bjorgan, K., During, M.J., Sprengel, R., Seeburg, P.H., and Nicoll, R.A. (2009). Subunit composition of synaptic AMPA receptors revealed by a single-cell genetic approach. Neuron *62*, 254–268.

Lu, W., Bushong, E.A., Shih, T.P., Ellisman, M.H., and Nicoll, R.A. (2013). The cell-autonomous role of excitatory synaptic transmission in the regulation of neuronal structure and function. Neuron *78*, 433–439.

Magee, J.C. (2000). Dendritic integration of excitatory synaptic input. Nat. Rev. Neurosci. *1*, 181–190.

Malewicz, M., Kadkhodaei, B., Kee, N., Volakakis, N., Hellman, U., Viktorsson, K., Leung, C.Y., Chen, B., Lewensohn, R., van Gent, D.C., et al. (2011). Essential role for DNA-PK-mediated phosphorylation of NR4A nuclear orphan receptors in DNA double-strand break repair. Genes Dev. *25*, 2031–2040.

Marin-Padilla, M. (1967). Number and distribution of the apical dendritic spines of the layer V pyramidal cells in man. J. Comp. Neurol. *131*, 475–490.

Matsuzaki, M., Honkura, N., Ellis-Davies, G.C., and Kasai, H. (2004). Structural basis of long-term potentiation in single dendritic spines. Nature *429*, 761–766.

Nägerl, U.V., Eberhorn, N., Cambridge, S.B., and Bonhoeffer, T. (2004). Bidirectional activity-dependent morphological plasticity in hippocampal neurons. Neuron *44*, 759–767.

Nakayama, A.Y., Harms, M.B., and Luo, L. (2000). Small GTPases Rac and Rho in the maintenance of dendritic spines and branches in hippocampal pyramidal neurons. J. Neurosci. *20*, 5329–5338.

Nimchinsky, E.A., Sabatini, B.L., and Svoboda, K. (2002). Structure and function of dendritic spines. Annu. Rev. Physiol. *64*, 313–353.

Pak, D.T., and Sheng, M. (2003). Targeted protein degradation and synapse remodeling by an inducible protein kinase. Science *302*, 1368–1373.

Pak, D.T., Yang, S., Rudolph-Correia, S., Kim, E., and Sheng, M. (2001). Regulation of dendritic spine morphology by SPAR, a PSD-95-associated RapGAP. Neuron *31*, 289–303.

Peck, J.W., Oberst, M., Bouker, K.B., Bowden, E., and Burbelo, P.D. (2002). The RhoA-binding protein, rhophilin-2, regulates actin cytoskeleton organization. J. Biol. Chem. *277*, 43924–43932.

Pi, H.J., Otmakhov, N., El Gaamouch, F., Lemelin, D., De Koninck, P., and Lisman, J. (2010). CaMKII control of spine size and synaptic strength: role of phosphorylation states and nonenzymatic action. Proc. Natl. Acad. Sci. USA *107*, 14437–14442.

Pulipparacharuvil, S., Renthal, W., Hale, C.F., Taniguchi, M., Xiao, G., Kumar, A., Russo, S.J., Sikder, D., Dewey, C.M., Davis, M.M., et al. (2008). Cocaine regulates MEF2 to control synaptic and behavioral plasticity. Neuron *59*, 621–633.

Ramirez-Herrick, A.M., Mullican, S.E., Sheehan, A.M., and Conneely, O.M. (2011). Reduced NR4A gene dosage leads to mixed myelodysplastic/myeloproliferative neoplasms in mice. Blood *117*, 2681–2690.

Sala, C., Piëch, V., Wilson, N.R., Passafaro, M., Liu, G., and Sheng, M. (2001). Regulation of dendritic spine morphology and synaptic function by Shank and Homer. Neuron *31*, 115–130.

Saneyoshi, T., Fortin, D.A., and Soderling, T.R. (2010). Regulation of spine and synapse formation by activity-dependent intracellular signaling pathways. Curr. Opin. Neurobiol. *20*, 108–115.

Seeburg, D.P., and Sheng, M. (2008). Activity-induced Polo-like kinase 2 is required for homeostatic plasticity of hippocampal neurons during epileptiform activity. J. Neurosci. *28*, 6583–6591.

Seeburg, D.P., Feliu-Mojer, M., Gaiottino, J., Pak, D.T., and Sheng, M. (2008). Critical role of CDK5 and Polo-like kinase 2 in homeostatic synaptic plasticity during elevated activity. Neuron *58*, 571–583.

Shankar, G.M., Bloodgood, B.L., Townsend, M., Walsh, D.M., Selkoe, D.J., and Sabatini, B.L. (2007). Natural oligomers of the Alzheimer amyloid-beta protein induce reversible synapse loss by modulating an NMDA-type glutamate receptor-dependent signaling pathway. J. Neurosci. *27*, 2866–2875.

Sheng, M., and Hoogenraad, C.C. (2007). The postsynaptic architecture of excitatory synapses: a more quantitative view. Annu. Rev. Biochem. *76*, 823–847.

Shepherd, G.M. (1996). The dendritic spine: a multifunctional integrative unit. J. Neurophysiol. *75*, 2197–2210.

Siddiqui, T.J., Tari, P.K., Connor, S.A., Zhang, P., Dobie, F.A., She, K., Kawabe, H., Wang, Y.T., Brose, N., and Craig, A.M. (2013). An LRRTM4-HSPG complex mediates excitatory synapse development on dentate gyrus granule cells. Neuron *79*, 680–695.

Tashiro, A., and Yuste, R. (2004). Regulation of dendritic spine motility and stability by Rac1 and Rho kinase: evidence for two forms of spine motility. Mol. Cell. Neurosci. *26*, 429–440.

Tolias, K.F., Bikoff, J.B., Burette, A., Paradis, S., Harrar, D., Tavazoie, S., Weinberg, R.J., and Greenberg, M.E. (2005). The Rac1-GEF Tiam1 couples the NMDA receptor to the activity-dependent development of dendritic arbors and spines. Neuron *45*, 525–538.

Volakakis, N., Kadkhodaei, B., Joodmardi, E., Wallis, K., Panman, L., Silvaggi, J., Spiegelman, B.M., and Perlmann, T. (2010). NR4A orphan nuclear receptors as mediators of CREB-dependent neuroprotection. Proc. Natl. Acad. Sci. USA *107*, 12317–12322.

von Hertzen, L.S., and Giese, K.P. (2005). Memory reconsolidation engages only a subset of immediate-early genes induced during consolidation. J. Neurosci. *25*, 1935–1942.

Wang, Z., Benoit, G., Liu, J., Prasad, S., Aarnisalo, P., Liu, X., Xu, H., Walker, N.P., and Perlmann, T. (2003). Structure and function of Nurr1 identifies a class of ligand-independent nuclear receptors. Nature *423*, 555–560.

Wang, X.B., Yang, Y., and Zhou, Q. (2007). Independent expression of synaptic and morphological plasticity associated with long-term depression. J. Neurosci. *27*, 12419–12429.

Wilson, T.E., Paulsen, R.E., Padgett, K.A., and Milbrandt, J. (1992). Participation of non-zinc finger residues in DNA binding by two nuclear orphan receptors. Science *256*, 107–110.

Woods, G.F., Oh, W.C., Boudewyn, L.C., Mikula, S.K., and Zito, K. (2011). Loss of PSD-95 enrichment is not a prerequisite for spine retraction. J. Neurosci. *31*, 12129–12138.

Yuste, R. (2011). Dendritic spines and distributed circuits. Neuron *71*, 772–781.

Zhang, S.J., Steijaert, M.N., Lau, D., Schütz, G., Delucinge-Vivier, C., Descombes, P., and Bading, H. (2007). Decoding NMDA receptor signaling: identification of genomic programs specifying neuronal survival and death. Neuron *53*, 549–562.

Zhang, S.J., Zou, M., Lu, L., Lau, D., Ditzel, D.A., Delucinge-Vivier, C., Aso, Y., Descombes, P., and Bading, H. (2009). Nuclear calcium signaling controls expression of a large gene pool: identification of a gene program for acquired neuroprotection induced by synaptic activity. PLoS Genet. *5*, e1000604.

Zhou, Q., Homma, K.J., and Poo, M.M. (2004). Shrinkage of dendritic spines associated with long-term depression of hippocampal synapses. Neuron *44*, 749–757.

Zito, K., Knott, G., Shepherd, G.M., Shenolikar, S., and Svoboda, K. (2004). Induction of spine growth and synapse formation by regulation of the spine actin cytoskeleton. Neuron *44*, 321–334.